Theoretical Study on the Mechanism of the Reaction of CH_4 + MgO

Chang-Wei Hu,*,† Hua-Qing Yang,† Ning-Bew Wong,*,‡ Yao-Qiang Chen,† Mao-Chu Gong,† An-Min Tian,† Can Li,§ and Wai-Kee Li⊥

Sichuan Key Laboratory of Green Chemistry and Technology, Faculty of Chemistry, Sichuan University, Chengdu, Sichuan 610064, People's Republic of China, Department of Biology and Chemistry, City University of Hong Kong, Kowloon, Hong Kong, State Key Laboratory of Catalysis, Dalian Institute of Chemical Physics, Chinese Academy of Sciences, Dalian, 116023, People's Republic of China, and Department of Chemistry, The Chinese University of Hong Kong, Shatin, N. T., Hong Kong

Received: August 23, 2002; In Final Form: December 17, 2002

The reactions of (1) CH_4 + MgO → $MgOH^•$ + $CH_3^•$ and (2) CH_4 + MgO → Mg + CH_3OH have been studied on the singlet spin state potential energy surface at the MP2/6-311+G(2d,2p) level. These two reaction channels, both involving intermediates and transition states, have been rationalized by the structures of the species involved, natural bond orbital (NBO), and vibrational frequency analysis. We have considered two initial interacting models between CH_4 and MgO: a collinear C−H approach to the O end of the MgO forming the $MgOCH_4$ complex with C_{3v} symmetry and three hydrogen atoms of the methane point to the Mg end of the MgO forming the $OMgCH_4$ complex with C_1 symmetry. The calculations predict that reactions 1 and 2 are exothermic by 39.8 and 86.5 kJ mol^{-1}, respectively. Also, the former reaction proceeds more easily than the latter, and the complex $HOMgCH_3$ is energetically preferred in the reaction of MgO + CH_4.

1. Introduction

Over the past few years, conversion of natural gas, mainly composed of methane, into more easily handled and stored products, such as methanol or ethylene, has been widely studied.[1] The partial oxidation and oxidative coupling of methane, in particular, have attracted considerable attention.[2−9] Many metal oxide catalysts have been used for these reactions,[2,10−12] and MgO has been found to be one of the most effective catalysts.[12,13]

To understand the nature of the interaction between methane and MgO, the adsorption and dissociation of methane on MgO catalyst have been extensively investigated experimentally.[2−6,10−18] In 1985, Driscoll and co-workers[10,11] found that when methane is passed over MgO at temperatures above 800 K, $CH_3^•$ radicals are formed, then released into the gas phase, and detected after collection in an argon matrix. Later, Ito and co-workers[15,16] proposed that methane pretreated above 973 K on MgO could be adsorbed in a heterolytically dissociated form, CH_3^- on Mg^{2+} and H^+ on O^{2-}, even below room temperature. Irrespective of the detailed mechanism of the coupling reaction, the dissociation of methane is generally accepted as the initial step in methane activation.[18] The rate-determining step in the conversion of methane to higher derivatives has been shown to be the abstraction of hydrogen at the surface.[4]

To obtain further information about this process, many theoretical studies of the interaction of methane with metal oxide heve been performed using an oxometal cluster model[9,16,18−21] and gaseous metal oxide molecules.[22−27] Of particular interest is the direct oxidation of methane by metal oxide fragments,[22−27] because this process can be justifiably regarded as providing models for the more complicated processes of heterogeneous or enzymatic methane monooxygenase catalysis. It is obvious that a better understanding of the details of the activation processes would be desirable in order to improve the catalysts. However, as far as we know, despite a few theoretical investigation of the C−H bond activation by bare MgO in the gas phase,[22,24] only the $CH_3^•$ radical formation from CH_4 was focused on, and the molecule−molecule interaction between CH_4 and MgO and the CH_3OH formation from CH_4 and MgO have not been studied.

In the present study, the following reactions are studied in detail at the MP2/6-311+G(2d,2p) level.

$$CH_4 + MgO \rightarrow MgOH^• + CH_3^•$$

$$CH_4 + MgO \rightarrow Mg + CH_3OH$$

2. Computational Details

Full-parametric geometry optimizations, final energy evaluation, and vibrational frequency calculations for all equilibrium structures and transition states were performed at the MP2/6-311+G(2d,2p) level using the Gaussian-98 program.[28] All vibrational frequencies were scaled by a factor of 0.943.[29] It should be noted that all transition states have been verified by the intrinsic reaction coordinate (IRC) analysis.

3. Results and Discussion

The total energies corrected by zero-point energy (ZPE) and relative energies of various species in the MgO + CH_4 reaction calculated at the MP2/6-311+G(2d,2p) theoretical level are listed in Table 1. The schematic energy diagram along the singlet reaction pathway using ZPE corrected relative energies of various species is shown in Figure 1. The optimized geometries of various species on the singlet potential energy curve of the

* Corresponding authors. E-mail Addresses: Chang-Wei Hu, chwehu@mail.sc.cninfo.net; Ning-Bew Wong, bhnbwong@cityu.edu.hk.
† Sichuan University.
‡ City University of Hong Kong.
§ Chinese Academy of Sciences.
⊥ The Chinese University of Hong Kong.

10.1021/jp021953h CCC: $25.00
Published on Web 03/06/2003

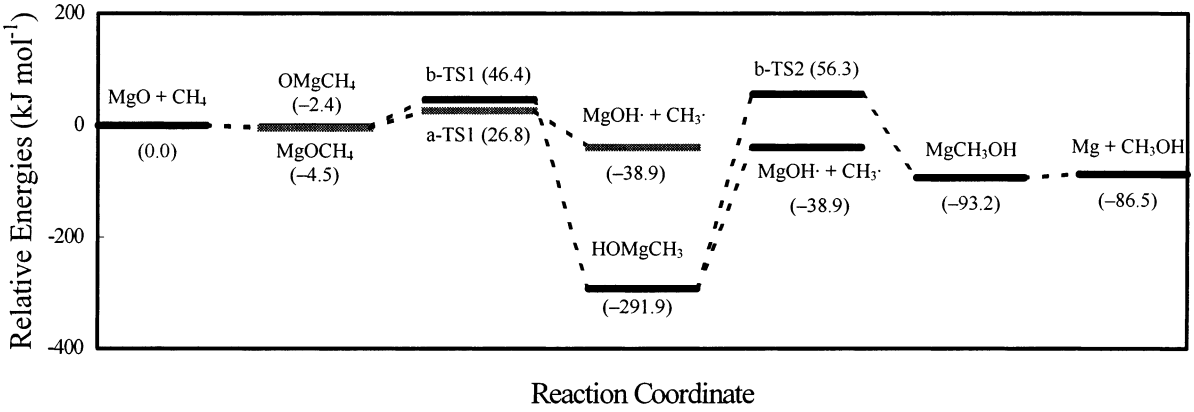

Figure 1. Potential energy profiles for the reaction between MgO + CH_4 at the MP2/6-311+G(2d,2p) level. Relative energies for the reactants, intermediates, transition states, and products relative to MgO + CH_4 are shown in parentheses.

TABLE 1: Total Energies (hartree) Corrected by Zero-Point Energy (ZPE) and Relative Energies E_r (kJ mol^{-1}) with Respect to Reactants [MgO($^1\Sigma$) + CH_4] Calculated at the MP2/6-311+G(2d,2p) Level of Theory of Various Species in the Reaction of CH_4 with MgO

species	total energy, hartree	E_r, kJ mol^{-1}
MgO($^1\Sigma$)	−274.67176	
CH4	−40.34808	
MgO($^1\Sigma$) + CH_4	−315.01984	0.0
$MgOCH_4$ (a-IM1)	−315.02226	−6.4
$MgOCH_4$ (a-IM1)[a]		−4.5
a-TS1	−315.00964	+26.8
$CH_3^•$	−39.69002	
MgOH$^•$	−275.34463	
MgOH$^•$ + $CH_3^•$	−315.03465	−38.9
$OMgCH_4$ (b-IM1)	−315.02185	−5.3
$MgOCH_4$ (a-IM1)[a]		−2.4
b-TS1	−315.00216	+46.4
$HOMgCH_3$ (b-IM2)	−315.13105	−291.9
CH_3^-	−39.68646	
$MgOH^+$	−275.07683	
CH_3^- + $MgOH^+$	−314.76329	+673.3
OH^-	−75.65512	
$MgCH_3^+$	−239.12276	
OH^- + $MgCH_3^+$	−314.77788	+635.0
b-TS2	−314.99837	+56.3
$MgCH_3OH$ (b-IM3)	−315.05536	−93.2
Mg	−199.62876	
CH_3OH	−115.42404	
Mg + CH_3OH	−315.05280	−86.5

[a] The relative energy corrected by basis sets superposition error (BSSE) with respect to reactants of MgO($^1\Sigma$) and CH_4.

MgO + CH_4 reaction are depicted in Figure 2. Atomic natural charges and atomic natural electron configurations, as well as dominant occupancies of natural bond orbital (NBO) and dominant stabilization energies $E(2)$ between donors and acceptors for various species by NBO analysis,[30,31] are presented in Tables 2−4, respectively. Table 5 lists the vibrational frequencies and corresponding IR intensities for reactants, intermediates and transition states.

As shown in Table 1, as well as in Figures 1 and 2, there are two different reaction channels when MgO reacts with methane, and the first one results in the generation of $CH_3^•$.

$$CH_4 + MgO \rightarrow MgOH^• + CH_3^• \quad (1)$$

The second reaction channel also results in the formation of $CH_3^•$, and it gives a clue to the formation of methanol as well. The overall reaction in this case is

$$CH_4 + MgO \rightarrow Mg + CH_3OH \quad (2)$$

In the following we will discuss these two reactions in depth.

3.1. Interaction between MgO and CH_4. In the $^1\Sigma$ ground state of MgO, the calculated Mg−O distance, 1.751 Å, is in good accord with the experimental value of 1.749 Å.[25] Additionally, both covalent and ionic contributions to the bonding are found from its atomic natural charges ($Mg^{+1.45}$ and $O^{-1.45}$) and 1.995 e occupancy of BD(σ)Mg−O. These results are in general agreement with those found in the literature.[20,22] The calculated dissociation energy (D_0) of the $^1\Sigma$ ground state of MgO, 283.0 kJ mol^{-1}, is close to the value of 246.6 ± 20.9 kJ mol^{-1} determined by Freiser and co-workers[32] from photodissociation experiments.

According to the vibrational analysis, the isolated CH_4 molecule is characterized by a triply degenerate C−H asymmetric stretching mode at 3028 cm^{-1} (ν_3) and by a nondegenerate C−H symmetric stretching mode at 2907 cm^{-1} (ν_1); the two degenerate H−C−H deformation modes are at 1505 cm^{-1} (ν_2) and 1293 cm^{-1} (ν_4). The symmetric stretching mode at 2907 cm^{-1} and the deformation mode at 1505 cm^{-1} are IR forbidden by symmetry but Raman active. These results are in good accord with literature.[17,18] These results indicate that the present theoretical method of MP2/6-311+G(2d,2p) is appropriate for the MgO + CH_4 system.

Two models concerning the initial interaction between CH_4 and MgO (Figures 1 and 2) are considered: (i) a collinear C−H approach to the O end of the Mg−O bond with the transferred hydrogen, in which the receiving oxygen and the methane carbon lined up ($MgOCH_4$ complex a-IM1 with C_{3v} symmetry), and (ii) three hydrogen atoms of the methane point to the Mg end of the Mg−O bond ($OMgCH_4$ complex b-IM1 with C_1 symmetry).

For both $MgOCH_4$ and $OMgCH_4$ molecule−molecule complexes, the MP2 basis set superposition errors (BSSE)[33] are only 1.9 and 2.9 kJ mol^{-1}, respectively, and CH_4 is loosely bound to MgO with small stabilization energies of 4.5 and 2.4 kJ mol^{-1}, respectively. As shown in Table 2, for the two complexes of $MgOCH_4$ and $OMgCH_4$, the total electronic charge of the CH_4 moiety or the MgO moiety is nearly neutral. These two interaction models of CH_4 interacting with MgO have not been reported in the literatures.[22,24,25] Nevertheless, they are consistent with experimental results.[17]

In the case of $MgOCH_4$ with C_{3v} symmetry, the C−H bond close to the O end of MgO is elongated by 0.003 Å, as compared to the uncomplexed C−H bond in the same complex. As shown in Table 4, the small stabilization energies of BD(σ)Mg−O → RY*(1)H(7) and BD(σ)C−H(7) → RY*(1)O indicate that there is a weak hyperconjugative interaction in Mg−O−H(7)−C. These weak effects correspond to a faint stabilization interaction, thus increasing the O−H interaction, making the molecule

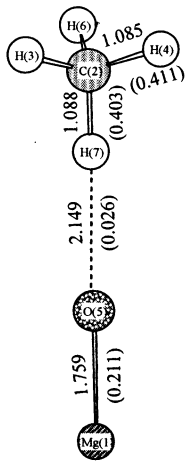

$MgOCH_4$
(C_{3v})

θ(3-2-1)=109.7
θ(4-2-1)=109.7
θ(5-2-1)=0.0
θ(6-2-1)=109.7
θ(7-2-1)=0.0
τ(4-2-1-3)=120.0
τ(5-2-1-3)=-164.8
τ(6-2-1-3)=-120.0
τ(7-2-1-3)=-160.0

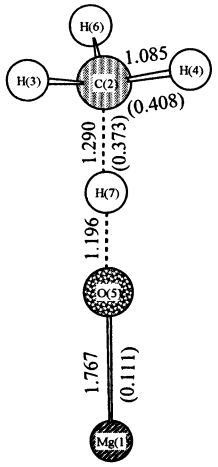

a-TS1
(C_{3v})

θ(3-2-1)=105.6
θ(4-2-1)=105.8
θ(5-2-1)=0.0
θ(6-2-1)=105.7
θ(7-5-2)=0.1
τ(4-2-1-3)=120.0
τ(5-2-1-3)=139.8
τ(6-2-1-3)=-120.0
τ(7-5-2-1)=0.0

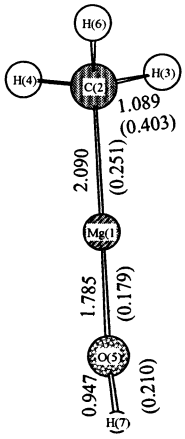

$HOMgCH_3$
(C_{3v})

θ(3-2-1)=111.5
θ(4-2-1)=111.7
θ(5-1-2)=179.5
θ(6-2-1)=111.5
θ(7-5-1)=178.8
τ(4-2-1-3)=120.0
τ(5-1-2-3)=0.3
τ(6-2-1-3)=-119.9
τ(7-5-1-2)=-107.0

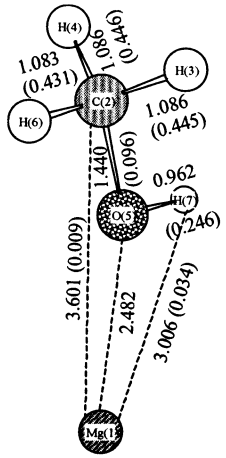

$MgCH_3OH$
(C_1)

θ(3-2-1)=108.3
θ(4-2-1)=135.1
θ(5-2-1)=31.1
θ(6-2-1)=78.7
θ(7-5-2)=109.1
τ(4-2-1-3)=147.5
τ(5-2-1-3)=101.1
τ(6-2-1-3)=-106.7
τ(7-5-2-1)=-152.1

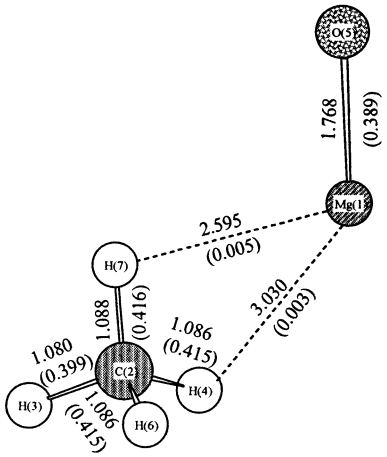

$OMgCH_4$
(C_1)

θ(3-2-1)=164.4
θ(4-2-1)=79.9
θ(5-1-2)=126.1
θ(6-2-1)=79.9
θ(7-5-1)=45.4
τ(4-2-1-3)=123.4
τ(5-1-2-3)=0.0
τ(6-2-1-3)=-123.4
τ(7-5-1-2)=0.0

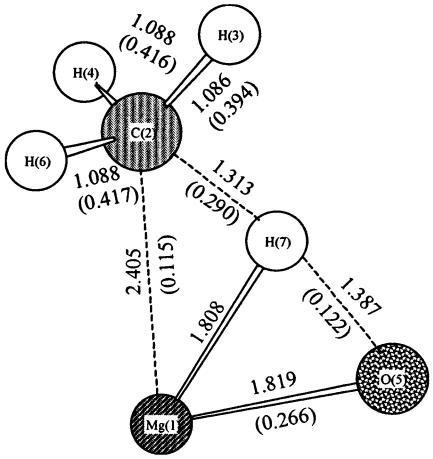

b-TS1
(C_1)

θ(3-2-1)=138.5
θ(4-2-1)=96.4
θ(5-1-2)=77.5
θ(6-2-1)=96.4
θ(7-5-1)=67.1
τ(4-2-1-3)=124.7
τ(5-1-2-3)=0.0
τ(6-2-1-3)=-124.8
τ(7-5-1-2)=0.0

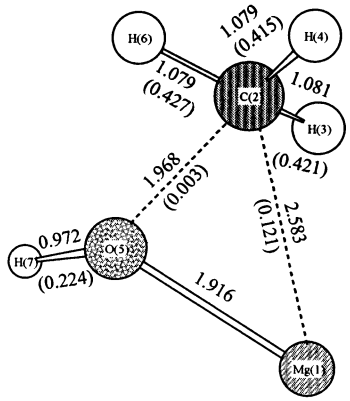

b-TS2
(C_1)

θ(3-2-1)=88.3
θ(4-2-1)=132.0
θ(5-1-2)=49.1
θ(6-2-1)=93.2
θ(7-5-1)=127.8
τ(4-2-1-3)=120.3
τ(5-1-2-3)=-138.9
τ(6-2-1-3)=-114.0
τ(7-5-1-2)=101.2

Figure 2. Calculated structures for the intermediates, transition states, and products involved in the potential energy profiles displayed in Figure 1. Bond lengths are in angstroms, bond angles (θ) and dihedral angles (τ) in degrees. The overlap populations from the Mulliken population analysis are in parentheses.

TABLE 2: Atomic Natural Charges and Atomic Natural Electron Configurations for Intermediates, Transition States and Products by Natural Bond Orbital Analysis

	Mg		C			H(3)		H(4)		O			H(6)		H(7)	
species	char.	3s	char.	2s	2p	char.	1s	char.	1s	char.	2s	2p	char.	1s	char.	1s
MgO	1.45	0.49								1.45	1.98	5.46				
CH_4			0.72	1.14	3.56	0.18	0.82	0.18	0.82				0.18	0.82	0.18	0.82
$MgOCH_4$	1.49	0.46	0.73	1.15	3.57	0.16	0.84	0.16	0.84	1.48	1.98	5.49	0.16	0.84	0.24	0.75
a-TS1	1.19	0.78	0.67	1.19	3.45	0.17	0.83	0.17	0.83	1.32	1.92	5.39	0.17	0.83	0.31	0.68
$CH_3^{\bullet}$			0.41	1.18	3.22	0.14	0.86	0.14	0.86				0.14	0.86		
$MgOH^{\bullet}$	1.00	0.88								1.49	1.82	5.62			0.49	0.51
$OMgCH_4$	1.53	0.42	0.77	1.15	3.60	0.22	0.78	0.18	0.82	1.53	1.98	5.54	0.18	0.82	0.19	0.81
b-TS1	1.57	0.40	1.07	1.22	3.82	0.24	0.76	0.17	0.83	1.42	0.94	5.46	0.17	0.83	0.34	0.65
$HOMgCH_3$	1.74	0.24	1.35	1.29	4.02	0.19	0.81	0.19	0.81	1.44	1.81	5.62	0.19	0.81	0.49	0.51
CH_3^-			1.34	1.26	3.99	0.11	0.89	0.11	0.89				0.11	0.89		
$MgOH^+$	1.95	0.02								1.48	1.83				0.53	0.47
OH^-										1.37	1.86	5.49			0.37	0.63
$MgCH_3^+$	1.47	0.53	1.11	1.27	3.81	0.21	0.78	0.21	0.78				0.21	0.78		
b-TS2	0.28	1.69	0.20	1.18	3.00	0.19	0.81	0.18	0.82	1.13	1.85	5.22	0.19	0.81	0.49	0.50
$MgCH_3OH$	0.02	1.97	0.10	1.07	3.00	0.14	0.85	0.14	0.85	0.85	1.70	5.12	0.16	0.84	0.48	0.51
CH_3OH			0.09	1.06	3.01	0.13	0.87	0.13	0.87				0.15	0.85	0.46	0.54

TABLE 3: Dominant Occupancies of Natural Bond Orbital for the Intermediates and Transition States by Natural Bond Orbital Analysis

	occupancy						
bond orbital	$MgOCH_4$	a-TS1	$OMgCH_4$	b-TS1	$HOMgCH_3$	b-TS2	$MgCH_3OH$
BD(σ)MgO	1.995	1.892	1.997	1.875			
BD(σ)MgC					1.996		
BD(σ)CH(3)	1.999	1.993	1.997	1.988	1.999	1.996	1.997
BD(σ)CH(4)	1.999	1.993	1.999	1.998	1.999	1.997	1.997
BD(σ)CO						1.996	1.999
BD(σ)CH(6)	1.999	1.993	1.999	1.998	1.999	1.996	1.994
BD(σ)CH(7)	1.993	1.703	1.997	1.910			
BD*(σ)MgO		0.307		0.114			
BD*(σ)CH(7)		0.166		0.220			
BD(σ)OH(7)					1.999	1.998	1.993
BD*(σ)MgC					0.039		
BD*(σ)CO						0.226	

TABLE 4: Dominant Stabilization Energies *E*(2) between Donors and Acceptors for Intermediates and Transition States by Natural Bond Orbital Analysis

species	donor	acceptor	$E(2)$, kJ mol^{-1}
$MgOCH_4$	BD(σ)MgO	RY*(1)H(7)	13.7
	BD(σ)CH(7)	RY*(1)O	1.6
a-TS1	LP(3)O	BD*(σ)MgO	55.5
	BD(σ)MgO	BD*(σ)CH(7)	252.1
	LP(3)O	BD*(σ)CH(7)	282.4
	BD*(σ)MgO	BD*(σ)CH(7)	88.7
	BD(σ)CH(7)	BD*(σ)MgO	395.9
$OMgCH_4$	BD(σ)MgO	BD*(σ)CH(3)	3.5
b-TS1	LP(3)O	BD*(σ)MgO	109.7
	BD(σ)MgO	BD*(σ)CH(7)	250.6
	LP(3)O	BD*(σ)CH(7)	342.2
	BD(σ)CH(7)	BD*(σ)MgO	144.5
$HOMgCH_3$	LP(3)O	BD*(σ)MgC	146.4
b-TS2	LP(1)Mg	RY*(1)O	104.6
	LP(1)Mg	BD*(σ)CO	186.7
$MgCH_3OH$	LP(1)Mg	RY*(1)O	32.5
	LP(1)O	RY*(1)Mg	7.4

complex $MgOCH_4$ stable. As shown in Table 5, according to the vibrational analysis, upon interaction of methane with an MgO molecule, frequencies of 3015 and 2995 cm^{-1}, which are assigned to the H−C−H asymmetric stretching modes of CH_4 moiety, and a frequency of 2882 cm^{-1}, which is assigned to the H−C−H symmetric stretching mode of the CH_4 moiety, are lower than those for free CH_4 (3028 and 2907 cm^{-1}). These indicate that the bonds of the CH_4 moiety have been weakly activated by the MgO molecule. The vibrational frequency of 3015 cm^{-1}, representative of the H−C−H asymmetric stretching mode of the CH_4 moiety in the $MgOCH_4$ complex, is 13 cm^{-1} lower than that for the free CH_4 molecule (3028 cm^{-1}). These results are in fairly good agreement with the experimental results (3008 vs 3019 cm^{-1} [17] and 3002 vs 3020 cm^{-1} [18]). Frequencies of 1505 and 1305 cm^{-1} are attributed to the H−C−H deformation modes of the CH_4 moiety, 1273 cm^{-1} to the convolution of the MgOH moiety stretching mode and CH_3 moiety deformation mode; 925 cm^{-1} to the convolution of MgO moiety stretching mode and CH moiety deformation mode, and 155, 102, and 41 cm^{-1} to the deformation modes of $MgOCH_4$.

As in the case of $OMgCH_4$, the C−H bonds of the three hydrogen atoms pointing to the Mg end of MgO are weakly elongated, as compared to the uncomplexed C−H bond. The molecule−molecule interaction of the two building blocks brings about an elongation of the Mg−O bond length by 0.017 Å, as compared with free MgO. The closest "complexed" hydrogen atom of methane, which is 2.595 Å away from the Mg atom, is to be abstracted preferentially upon collisional activation. This is to be borne out in the reaction as it proceeds. Based on the very small stabilization energy of BD(σ)Mg−O → BD*(σ)C−H(3) in the NBO results, there appears to be a very weak interaction between MgO and CH_4. According to the vibrational analysis of $OMgCH_4$ in Table 5, frequencies of 3018, 3006, and 2989 cm^{-1}, which are assigned to the asymmetric stretching modes of CH_4 moiety, and frequency of 2878 cm^{-1}, which is assigned to the symmetric stretching mode of CH_4 moiety, are lower than those in free CH_4 (3028 and 2907 cm^{-1}). These indicate that the bonds of the CH_4 moiety have been weakly activated by the MgO molecule. The vibrational frequency of 3018 cm^{-1}, representative of the H−C−H asymmetric stretching mode of the CH_4 moiety in the $OMgCH_4$ complex, is 10 cm^{-1} lower than those for free CH_4 molecule (3028 cm^{-1}). These results are in fairly good agreement with the experimental results

TABLE 5: Calculated Vibrational Frequencies and IR Intensities for All the Species Involved in the Reaction between MgO and CH_4

species	frequencies, cm^{-1}/IR intensities, $Debye^2\ amu^{-1}\ Å^{-2}$											
CH_4	1293/11.8	1293/11.8	1293/11.8	1505/0.0	1505/0.0	2907/0.0	3028/17.9	3028/17.9	3028/17.9			
$MgOCH_4$	41/63.4	41/63.4	102/0.0	155/1.3	155/1.3	925/1054	1273/13.7	1305/4.2	1305/4.2	1505/0.8	1505/0.8	2882/6.2	2995/0.2	3015/26.1	3015/26.1
a-TS1	1686i/5600	99/54.9	99/54.9	407/11.4	407/11.4	436/3.51	939/1583	1132/310	1136/12.2	1136/12.8	1381/1.6	1381/1.6	2910/90.0	3031/17.8	3031/17.8
$OMgCH_4$	30/ 64.8	46/10.9	55/24.3	78/0.0	178/6.6	883/522	1277/32.7	1298/12.5	1300/16.3	1501/7.2	1509/5.2	1509/5.2	2878/16.9	2989/4.5	3006/2.9	3018/11.9
b-TS1	1362i/1973	87/9.3	215/66.1	407/3.5	496/37.3	670/57.7	707/61.7	1163/35.6	1222/0.1	1367/1.3	1404/5.1	1404/5.1	1694/48.1	2903/5.78	2991/5.6	2999/0.5
$HOMgCH_3$	82/173.9	82/173.9	135/1.1	135/1.2	456/0.2	550/83.5	550/83.5	760/156.4	1104/0.9	1392/0.3	1392/0.3	1392/0.3	2889/17.0	2972/14.7	2973/14.6	3841/90.2
b-TS2	749i/3000	130/0.8	242/23.9	281/95.3	523/12.3	606/52.2	710/45.5	805/184.8	1042/16.9	1385/35.6	1396/5.2	2953/25.7	3069/43.5	3087/1.0	3492/21.0
$MgCH_3OH$	39/8.4	70/3.2	104/13.0	273/71.5	960/105.6	1023/25.6	1116/1.1	1295/25.0	1415/6.6	1442/3.6	1454/8.6	2916/43.5	2995/16.8	3027/8.1	3619/44.2
CH_3OH	277/113.7	991/114.6	1032/3.4	1123/0.5	1309/21.5	1422/3.8	1446/3.0	1457/4.8	2892/53.3	2956/43.0	3015/20.5	3671/39.8			

(3008 vs 3019 cm^{-},[117] and 3002 vs 3020 cm^{-1}[118]). Frequencies of 1509, 1501, 1300, 1298, and 1277 cm^{-1} are ascribed to the deformation modes of the CH_4 moiety, 883 cm^{-1} to the convolution of the MgO moiety stretching mode and C−H moiety deformation mode, and 178, 78, 55, 46, and 30 cm^{-1} to the deformation modes of $OMgCH_4$.

3.2. First Reaction Channel: MgO + CH_4 → MgOH$^{\bullet}$ + $CH_3^{\bullet}$ via a-TS1. This reaction is composed of two steps. As mentioned previously, the first step is the formation of molecule−molecule complex $MgOCH_4$.

$$CH_4 + MgO \rightarrow MgOCH_4 \tag{3}$$

The second step involves a C−H bond cleavage, yielding the products MgOH$^{\bullet}$ + $CH_3^{\bullet}$ via a transition state a-TS1.

$$MgOCH_4 \rightarrow \text{a-TS1} \rightarrow MgOH^{\bullet} + CH_3^{\bullet} \tag{4}$$

In this step, there are an activation energy of 31.3 kJ mol^{-1} and an exothermicity of 34.4 kJ mol^{-1}. Such a low activation energy makes this step proceed easily, and thus gas-phase methyl radicals have been observed when methane was passed over MgO at appropriate temperatures.[6,10,11] This activation barrier is not far from that obtained by the CCI+Q method in the literature (45.6 kJ mol^{-1}),[22] although it is markedly lower than that obtained by the semiempirical method in a previous study (130.0 kJ mol^{-1}).[24] The formation of MgOH$^{\bullet}$ and $CH_3^{\bullet}$ is exothermic by 38.9 kJ mol^{-1} with respect to the reactants CH_4 + MgO. This result is in agreement with experimental value (29.7 kJ mol^{-1})[22,25] and the theoretical result (33.4 kJ mol^{-1}) by the more sophisticated CCI+Q calculations,[22] although it is considerably less than that obtained by the semiempirical method in the literature (74.0 kJ mol^{-1}).[24]

For the transition state a-TS1, the O−H(7) distance is exceedingly shorter, and the C−H(7) distance becomes considerably longer and the Mg−O slightly longer, than the corresponding distances in $MgOCH_4$. These results indicate that the C−H(7) and Mg−O bonds have been weakened and the interaction O−H(7) has been strengthened. The transition state, a-TS1, could be described as being "late" because the C−H bond is almost broken and the transference of the hydrogen atom to the oxygen atom is almost complete. Børve et al.[22] and Stiakaki et al.[24] also studied the model of CH_4 interacting with the O end of MgO and found that the reactants proceed directly to the corresponding transition state, without passing through the molecule−molecule complex of MgO and CH_4. Børve et al.[22] kept the CH_3 fragment rigid at the SCF, CASSCF, and CCI+Q levels and found a similar transition state as that presented above, in which the O−H(7) and C−H(7) distances are 1.31 and 1.22 Å, respectively. Stiakaki et al.[24] adopted full optimization and carried out semiempirical PM3 and MNDO methods and found the transition state, in which the Mg, O, H and C atoms are not linearly arranged. Obviously, in the present study the structure of the transition state a-TS1 is close to that obtained by Børve et al.[22] and completely different from that obtained by Stiakaki et al.[24] As shown in Table 3, the occupancies of antibond orbitals [0.166 e for BD*(σ)C−H(7) and 0.307 e for BD*(σ)Mg−O] underline that both C−H(7) and Mg−O bonds are weakened. As shown in Table 4, the large stabilization energies [BD(σ)C−H(7) → BD*(σ)Mg−O, LP-(3)O → BD*(σ)C−H(7), and BD(σ)Mg−O → BD*(σ)C−H(7)] emphasize that the dominant hyperconjugative interaction in Mg−O−H−C may increase the interaction of O−H(7) and weaken the interactions of Mg−O and C−H(7). As shown in Table 5, the vibrational trend of the unique imaginary frequency

of 1686i cm^{-1} is that H(7) gets gradually closer to O and farther away from C. This stresses that the transition state a-TS1 could be described as "late", thus the C−H(7) bond is going to rupture and the O−H(7) bond is ready to form.

From Table 2, it can be seen that a total electronic charge amounting to 0.13 e is transferred from the methane moiety to the MgO moiety in the transition state a-TS1. This charge transfer is reflected in both the lower net positive charge on the Mg atom and the higher net negative charge on the O atom, when compared with those of the isolated MgO molecule. Moreover, an appreciable positive net charge is accumulated at the H(7) atom, which is to be abstracted. According to the above results, it is apparent that the abstraction reaction proceeds by the formation of a three-center two-electron bond (3c−2e) between oxygen, hydrogen, and carbon centers. This 3c−2e bond then becomes the O−H bond in the product hydroxide.

3.3. Second Reaction Channel: $MgO + CH_4 \rightarrow Mg + CH_3OH$ and $MgOH^{\bullet} + CH_3^{\bullet}$. This reaction channel can be divided into several steps, as described in eqs 5−8. In the first step, the reactants form molecule−molecule complex $OMgCH_4$.

$$CH_4 + MgO \rightarrow OMgCH_4 \qquad (5)$$

The next step is an oxidative addition, cleaving the C−H bond and yielding an insertion product $HOMgCH_3$ via the transition state b-TS1. The intermediate $HOMgCH_3$ represents the absolute minimum of the potential energy curve.

$$OMgCH_4 \rightarrow \text{b-TS1} \rightarrow HOMgCH_3 \qquad (6)$$

This step involves an activation energy of 48.8 kJ mol^{-1} and a massive exothermicity of 289.5 kJ mol^{-1}. This activation barrier is close to the value (43.7 kJ mol^{-1}) obtained on the interaction of methane with the Mg_4O_4 cluster model by Ito et al.[16] The formation of $HOMgCH_3$ is exothermic by 291.9 kJ mol^{-1} with respect to the reactants CH_4 + MgO.

For the transition state b-TS1, with C_1 symmetry, the Mg−C and O−H(7) distances are remarkably shorter than those for $OMgCH_4$, while their overlap populations are larger. The C−H(7) and Mg−O distances are longer than those for $OMgCH_4$, while their overlap populations are smaller. This indicates that the interactions of Mg−C and O−H(7) have been reinforced and the C−H(7) and Mg−O bonds have been activated. The transition state, b-TS1, could be best characterized as an "early" transition state, since the O−H(7) bond is only partially formed and the C−H(7) bond is ruptured only to a small degree. As shown in Table 3, the occupancies of antibond orbitals [0.220 e for BD*(σ)C−H(7) and 0.114 e for BD*(σ)-Mg−O] underline that both C−H(7) and Mg−O bonds are weakened. As shown in Table 4, the large stabilization energies [BD(σ)Mg−O → BD*(σ)C−H(7), BD(σ)C−H(7) → BD*(σ)-Mg−O, LP(3)O → BD*(σ)C−H(7), and LP(3)O → BD*(σ)-Mg−O] indicate that the dominant hyperconjugative interaction exists in the Mg−O−H−C four-membered ring. Subsequently, this effect may increase the interactions of O−H(7) and Mg−C and weaken the interactions of Mg−O and C−H(7). The vibrational trend of the unique imaginary frequency of 1362i cm^{-1} is that H(7) gets gradually closer to C and farther away from O. This underlines that the transition state b-TS1 could be described as "early". According to atomic natural charges of the transition state b-TS1, there is a charge transfer from Mg to C and from H of the C−H bond to cleave the O atom, and afterward it results in a transfer of 0.15 e from MgO moiety to the CH_4 moiety. Consequently, the contribution of covalent stabilization of the four-center four-electron metallocycle accounts for the stability of the transition state b-TS1, which is reflected in the low activation barrier.

For $HOMgCH_3$, both O−H(7) and Mg−C distances are remarkably shorter than those for the transition state b-TS1, while their overlap populations are considerably larger. These are the characteristics of the Mg−C and O−H(7) single bonds, which are verified in Table 3 by the occupancies of 1.966 and 1.999 e for BD(σ)Mg−C and BD(σ)O−H(7), respectively. As shown in Figure 2, the C−H(7) distance is prominently longer than that in the transition state b-TS1, indicating that the C−H(7) bond has been completely cleaved. This intermediate, $HOMgCH_3$, which formally corresponds to the insertion product of Mg in the C−O bond of methanol, can be viewed as the result of a σ-methathesis process between a C−H bond of methane and an Mg−O bond, followed by structural relaxation to yield the species with C_{3v} symmetry. The structure of $HOMgCH_3$ is similar to that of $HOFeCH_3^+$ in the dissociation of CH_4 on FeO^+ reaction.[23] From the atomic natural charges in Table 2, the electronic features support the view that $HOMgCH_3$ can be described as either CH_3^- interacting with $MgOH^+$ or OH^- interacting with $MgCH_3^+$, since both the CH_3 and OH moieties are close to −1 valence and both MgOH and $MgCH_3$ moieties are close to +1 valence. These interactions are so large that the $HOMgCH_3$ molecule is especially stable. This can also be afforded by the exceedingly large dissociation energies (965.2 and 926.9 kJ mol^{-1}) in the formations of $CH_3^- + MgOH^+$ and $OH^- + MgCH_3^+$ from the $HOMgCH_3$ molecule, respectively. This holds true, in particular, for the $HOMgCH_3$ molecule residing in a deep potential well. This model of CH_3^- interacting with $MgOH^+$ is similar to that proposed by Ito et al.[15,16] As shown in Table 4, the large stabilization energy for LP(3)O → BD*(σ)Mg−C indicates that there is a large hyperconjugative interaction in O−Mg−C and subsequently accounts for the stable $HOMgCH_3$ molecule. Therefore, the intermediate $HOMgCH_3$ is predicted to be the energetically preferred configuration in the gas-phase reaction of MgO + CH_4. According to the vibrational analysis, the frequency of 3841 cm^{-1} is assigned to the O−H stretching mode, 2973, 2972, and 2889 cm^{-1} to the asymmetric stretching modes of CH_3 moiety, 1392, 1104, and 550 cm^{-1} to the deformation modes of CH_3 moiety, 760 and 456 cm^{-1} to the stretching modes of $HOMg-CH_3$, and 135 and 82 cm^{-1} to the deformation modes of $HOMgCH_3$.

The third step of the reaction under study is a reductive elimination leading to an atom−molecule complex $MgCH_3OH$ where a methanol is weakly bound to Mg via the transition state b-TS2.

$$HOMgCH_3 \rightarrow \text{b-TS2} \rightarrow MgCH_3OH \qquad (7)$$

For this step, the activation energy is 348.2 kJ mol^{-1} and there is an endothermicity of 198.7 kJ mol^{-1}. This large potential barrier separates $HOMgCH_3$ from the elimination products of CH_3OH and Mg, and it indicates that the third step is the rate-determining step of the whole reaction. The formation of the $MgCH_3OH$ complex is similar to that of other metal complexes such as $FeCH_3OH^+$ [23] and $PtCH_3OH^+$ [34] from the corresponding insertion step.

For the transition state b-TS2, both the Mg−C and Mg−O distances are longer and the C−O one is shorter than those in $HOMgCH_3$. It appears that the bonds of Mg−C and Mg−O have been weakened and the C−O bond is being formed. This can be confirmed in Table 3 by the emerging of 1.996 e occupancy for BD(σ)C−O. Synchronously, the C−O bond has been activated according to the 0.226 e occupancy for antibond BD*(σ)C−O. The transition state, b-TS2, could be best

characterized as "early" transition state, since the C−O bond is only partially formed and Mg−O bond is only slightly ruptured. As shown in Table 4, the large stabilization energies in LP(1)Mg → RY*(1)O and LP(1)Mg → BD*(σ)C−O indicate that there is a dominant hyperconjugative interaction in the Mg−C−O three-membered ring. Subsequently, this effect may increase the interatomic interaction in Mg−O and weaken the interatomic interaction in C−O. The transition vector of the unique imaginary frequency of 749i cm^{-1} indicates that the CH_3 moiety moves gradually away from OH moiety. This implies that the transition state b-TS2 can be described as "early." According to atomic natural charges of the transition state b-TS2, there is a charge transfer from O and C to Mg as compared to those of $HOMgCH_3$, and afterward it results in a transfer of 1.15 e from the CH_3 moiety to the MgOH moiety as compared to that of $HOMgCH_3$. According to the above results, it is apparent that the elimination reaction proceeds by the formation of a three-center, two-electron (3c−2e) bond between the O, Mg, and C centers. This 3c−2e bond becomes the C−O bond in the product methanol.

The structure of $MgCH_3OH$ with C_1 symmetry is unlike that of Mg^+CH_3OH with C_s symmetry.[35] For $MgCH_3OH$, both C−O and O−H(7) distances are considerably shorter than those for the transition state b-TS2, whereas the Mg−C and Mg−O distances become distinctly longer. It appears that the C−O and O−H(7) bonds have been formed, and the Mg−C and Mg−O bonds have been entirely broken. These results can be verified in Table 3 by the occupancies of 1.999 and 1.993 e for BD(σ)C−O and BD(σ)O−H(7), respectively, and by the absence of occupancies for BD(σ)Mg−C and BD(σ)Mg−O. This complex could be regarded as the result of the interaction of methanol molecules with Mg atoms, according to the atomic natural charge of $MgCH_3OH$ (0.02 for Mg and −0.02 for CH_3-OH) in Table 2. In this species, complexation of methanol by the Mg atom does not significantly alter the geometry of the organic part; only the C−O bond is elongated by 0.013 Å, as compared to free CH_3OH molecule. As shown in Table 4, the comparatively small stabilization energies of LP(1)Mg → RY*(1)O and LP(1)O → RY*(1)Mg indicate that the Mg atom interacts weakly with the O end of the CH_3OH molecule.

For the free CH_3OH molecule, according to the vibrational analysis, the vibrational frequency of 3671 cm^{-1} is attributed to the O−H stretching mode, 3015 and 2956 cm^{-1} to the asymmetric stretching modes of the CH_3 moiety, 2892 cm^{-1} to the symmetric stretching mode of CH_3 moiety, 1457, 1446, 1422, and 1123 cm^{-1} to the deformation modes of CH_3 moiety, and 1309, 1032, 991, and 277 cm^{-1} to the deformation modes of CH_3OH.

As shown in Table 5, for $MgCH_3OH$, the vibrational frequency of 3619 cm^{-1}, which is assigned to the O−H stretching mode, is reduced by 52 cm^{-1}, as compared to that of free methanol molecule (3671 cm^{-1}). It is apparent that the O−H bond in CH_3OH has been activated by the Mg atom. Meanwhile, frequencies of 3027 and 2995 cm^{-1} are ascribed to the asymmetric stretching modes of the CH_3 moiety, 2916 cm^{-1} to the symmetric stretching mode of CH_3 moiety, 1454, 1442, 1415, and 1116 cm^{-1} to the deformation modes of CH_3 moiety, 1295, 1023, 960, and 273 cm^{-1} to the deformation modes of CH_3OH moiety, and 104, 70, and 39 cm^{-1} to the deformation modes of $MgCH_3OH$.

The final step is the release of the methanol molecule, leaving the magnesium atom behind at a very low cost of 6.7 kJ mol^{-1}.

$$MgCH_3OH \rightarrow Mg + CH_3OH \qquad (8)$$

The MgO reaction with methane to form $Mg + CH_3OH$ is exothermic by 86.5 kJ mol^{-1}. Furthermore, the calculated results strongly suggest that the possibility of MgO reacting with CH_4 proceeding all way to form CH_3OH and Mg is highly unlikely when the barrier to reductive elimination is considered. The calculations find the transition state b-TS2 lies 142.8 kJ mol^{-1} higher than the final products and 56.3 kJ mol^{-1} above the reactants. Thus, MgO does not react with methane to produce CH_3OH under the experimental condition reported.[19] Nevertheless, the formation of $HOMgCH_3$ from $MgO + CH_4$ is predicated to be possible.

Computational information is available for the reaction path following the $HOMgCH_3$ by simple bond cleavage, leaving $MgOH^\bullet + CH_3^\bullet$ as end products with an endothermicity of 253.0 kJ mol^{-1}. As mentioned above, the formation of $MgCH_3OH$ from $HOMgCH_3$ requires an energy barrier of 348.2 kJ mol^{-1}. Comparison of these energy barriers indicates that the reaction of $HOMgCH_3 \rightarrow MgOH^\bullet + CH_3^\bullet$ is easier to occur. In other words, the reaction proceeding all way to CH_3OH elimination becomes highly unlikely when the high barrier is considered.

4. Summary

The following key points may be made from the results presented here.

Concerning the initial interaction between CH_4 and MgO, two interaction models are proposed: (i) a collinear C−H approach to the O end of the Mg−O bond with the transferred hydrogen, in which the receiving oxygen and the methane carbon lined up ($MgOCH_4$ complex with C_{3v} symmetry), and (ii) three hydrogen atoms of the methane point to the Mg end of the Mg−O bond ($OMgCH_4$ complex with C_1 symmetry).

The reactions of $CH_4 + MgO \rightarrow MgOH^\bullet + CH_3^\bullet$ and $CH_4 + MgO \rightarrow Mg + CH_3OH$ are exothermic by 38.9 and 86.5 kJ mol^{-1} at the MP2/6-311+G(2d, 2p) level, respectively. The former reaction proceeds more easily than the latter. The complex $HOMgCH_3$ is predicted to be the energetically preferred configuration in the reaction of $MgO + CH_4$.

Acknowledgment. The authors from Chengdu are grateful for financial support by the Key Project of National Fundamental Research and Development of China (973) (No. G1999022407), NNSF (No. 29873028), the Special Research Foundation of Doctoral Education of China (No. 2000061028), and the Foundation of Science and Technology of Sichuan Province (No. 200018-16). N.B.W. thanks the City University of Hong Kong for the award of a Strategic Grant (Account No. 7001351).

References and Notes

(1) Keller, G. E.; Bhasin, M. M. *J. Catal.* **1982**, *73*, 9.
(2) Ito, T.; Wang, J.-X.; Lin, C. H.; Lunsford, J. H. *J. Am. Chem. Soc.* **1985**, *107*, 5062.
(3) Fujimoto, K.; Hashimoto, S.; Asami, K.; Tominaga, H. *Chem. Lett.* **1987**, 2157.
(4) Cant, N. W.; Lukey, C. A.; Nelson, P. F.; Tyler, R. J. *J. Chem. Soc., Chem. Commun.* **1988**, 766.
(5) Nelson, P. F.; Lukey, C. A.; Cant, N. W. *J. Phys. Chem.* **1988**, *92*, 6176.
(6) Tong, Y.; Lunsford, J. H. *J. Chem. Soc., Chem. Commun.* **1990**, 792.
(7) Lunsford, J. H.; Yang, X.; Haller, K.; Laane, J. *J. Phys. Chem.* **1993**, *97*, 13 810.
(8) Mims, C. A.; Mauti, R.; Dean, A. M.; Rose, K. D. *J. Phys. Chem.* **1994**, *98*, 13 357.
(9) Johnson, M. A.; Stefanovich, E. V.; Truong, T. N. *J. Phys. Chem. B* **1997**, *101*, 3196.
(10) Driscoll, D. J.; Lunsford, J. H. *J. Phys. Chem.* **1985**, *89*, 4415.
(11) Driscoll, D. J.; Martir, W.; Wang, J.-X.; Lunsford, J. H. *J. Am. Chem. Soc.* **1985**, *107*, 58.
(12) Ito, T.; Lunsford, J. H. *Nature* **1985**, *314*, 721.

(13) Lin, C. H.; Ito, T.; Wang, J.; Lunsford, J. H. *J. Am. Chem. Soc.* **1987**, *109*, 4808.
(14) Aika, K.; Lunsford, J. H. *J. Phys. Chem.* **1977**, *81*, 1393.
(15) Ito, T.; Tashiro, T.; Watanabe, T.; Toi, K.; Ikemoto, I. *Chem. Lett.* **1987**, 1723.
(16) Ito, T.; Tashiro, T.; Kawasaki, M.; Watanabe, T.; Toi, K.; Kobayashi, H. *J. Phys. Chem.* **1991**, *95*, 4476.
(17) Li, C.; Li, G.; Xin Q. *J. Phys. Chem.* **1994**, *98*, 1933.
(18) Ferrari, A. M.; Huber, S.; Knözinger, H.; Neyman, K. M.; Rösch, N. *J. Phys. Chem. B* **1998**, *102*, 4548.
(19) Mehandru, S. P.; Anderson, A. B.; Brazdil, J. F. *J. Am. Chem. Soc.* **1988**, *110*, 1715.
(20) Børve, K. J.; Pettersson, L. G. M. *J. Phys. Chem.* **1991**, *95*, 7401.
(21) Anchell, J. L.; Morokuma, K.; Hess, A. C. *J. Chem. Phys.* **1993**, *99*, 6004.
(22) Børve, K.; Pettersson, L. G. M. *J. Phys. Chem.* **1991**, *95*, 3214.
(23) Schröder, D.; Fiedler, A.; Hru×f0ák, J. Schwarz, H. *J. Am. Chem. Soc.* **1992**, *114*, 1215.
(24) Stiakaki, M.-A. D.; Tsipis, A. C.; Tsipis, C. A.; Xanthopoulos, C. E. *J. Mol. Catal.* **1993**, *82*, 425.
(25) Aray, Y.; Rodríguez, J.; Murgich, J.; Ruette, F. *J. Phys. Chem.* **1993**, *97*, 8393.
(26) Stiakaki, M.-A. D.; Tsipis, A. C.; Tsipis, C. A.; Xanthopoulos, C. E. *New. J. Chem.* **1994**, *18*, 203.
(27) Broclawik, E.; Haber, J.; Endou, A.; Stirling, A.; Yamauchi, R.; Kubo, M.; Miyamoto, A. *J. Mol. Catal. A* **1997**, *119*, 35.
(28) Frisch, M. J.; Trucks, G. W.; Schlegel, H. B.; Scuseria, G. E.; Robb, M. A.; Cheeseman, J. R.; Zakrzewski, V. G.; Montgomery, J. A., Jr.; Stratmann, R. E.; Burant, J. C.; Dapprich, S.; Millam, J. M.; Daniels, A. D.; Kudin, K. N.; Strain, M. C.; Farkas, O.; Tomasi, J.; Barone, V.; Cossi, M.; Cammi, R.; Mennucci, B.; Pomelli, C.; Adamo, C.; Clifford, S.; Ochterski, J.; Petersson, G. A.; Ayala, P. Y.; Cui, Q.; Morokuma, K.; Malick, D. K.; Rabuck, A. D.; Raghavachari, K.; Foresman, J. B.; Cioslowski, J.; Ortiz, J. V.; Stefanov, B. B.; Liu, G.; Liashenko, A.; Piskorz, P.; Komaromi, I.; Gomperts, R.; Martin, R. L.; Fox, D. J.; Keith, T.; Al-Laham, M. A.; Peng, C. Y.; Nanayakkara, A.; Gonzalez, C.; Challacombe, M.; Gill, P. M. W.; Johnson, B. G.; Chen, W.; Wong, M. W.; Andres, J. L.; Head-Gordon, M.; Replogle, E. S.; Pople, J. A. *Gaussian 98*, revision A.7; Gaussian, Inc.: Pittsburgh, PA, 1998.
(29) Pople, J. A.; Scott, A. P.; Wong, M. W.; Radom, L. *Isr. J. Chem.* **1993**, *33*, 345.
(30) Reed, A. E.; Curtiss, L. A.; Weinhold, F. *Chem. Rev.* **1988**, *88*, 899.
(31) Reed, A. E.; Weinstock, R. B.; Weinhold, F. *J. Chem. Phys.* **1985**, *83*, 735.
(32) Operti, L.; Tews, E. C.; Macmahon, T. J.; Freiser, B. S. *J. Am. Chem. Soc.* **1989**, *111*, 9152.
(33) Boys, S. F.; Berrardi, F. *Mol. Phys.* **1970**, *19*, 553.
(34) Pavlov, M.; Blomberg, R. A.; Sieghbahn, E. M.; Wesendrup, R.; Heinemann, C.; Schwarz, H. *J. Phys. Chem. A* **1997**, *101*, 1567.
(35) Andersen, A.; Muntean, F.; Walter, D.; Rue, C.; Armentrout, P. B. *J. Phys. Chem. A* **2000**, *104*, 692.